An Analysis of Excitation of Magnetostatic Surface Waves in an In-Plane Magnetized YIG Film by the Integral Kernel Expansion Method

Yoshiaki Ando, *Member, IEEE*, Ning Guan, *Member, IEEE*, Ken'ichiro Yashiro, *Member, IEEE*, Sumio Ohkawa, *Senior Member, IEEE*, and Masashi Hayakawa

***Abstract*—We present a method to solve a kind of integral equations (we call it the integral kernel expansion method), and apply it to an analysis of excitation of magnetostatic surface-wave/magnetostatic backward-volume-wave modes in a magnetized yttrium–iron–garnet film. The Fourier integral of a normal component of magnetic flux density is derived in terms of an unknown current density flowing in a microstrip transducer. The integral kernel is expanded into a series of the Legendre polynomials and expansion of the unknown current density in terms of appropriate functions reduces the Fourier integral to a system of linear equations with unknown coefficients. Determination of the unknown coefficients allows us to estimate the power of magnetostatic waves, which characterizes the excitation. It is found that our numerical method is superior to the previous conventional method based on an assumed current density. In order to verify the validity of our method, we compare our results with the corresponding experiments, and we have found good agreement between the two.**

***Index Terms*—Integral equation, magnetostatic wave (MSW).**

I. Introduction

In this paper, we present a method to solve a kind of integral equation, which we call the integral kernel expansion method. As one of the applications of this method, we analyze the excitation of magnetostatic surface-wave (MSSW)/magnetostatic backward-volume-wave (MSBVW) modes in a magnetized yttrium–iron–garnet (YIG) film.

The integral kernel expansion method, which has been developed by our group [1]–[3], is appropriate in solving the mixed boundary-value problems, in which the field is formally expressed in terms of an integral transform including an unknown quantity at some parts of the boundary and, on the other hand, known at the remaining parts. Therefore, we obtain the integral-transform equation that the unknown quantity must satisfy. The integral kernel is expanded into a series of orthogonal polynomials over the parts of the boundary where the field is known. We then expand the unknown field into a series of proper functions, which reduces the integral equation to a system of linear equations with unknown coefficients.

Manuscript received December 18, 2002; revised August 28, 2002.

Y. Ando and M. Hayakawa are with the Department of Electronic Engineering, The University of Electro-Communications, Tokyo 182-8585, Japan.

N. Guan is with the Optics and Electronics Laboratory, Fujikura Ltd., Chiba 285-8550, Japan.

K. Yashiro and S. Ohkawa are with the Department of Electrical and Electronics Engineering, Chiba University, Chiba 263-8522, Japan.

Digital Object Identifier 10.1109/TMTT.2002.807827

The purpose of this paper is to apply our method to the analysis of the excitation of MSSWs in the YIG film magnetized obliquely. Magnetostatic waves (MSWs), which propagate in a magnetized YIG film, have potential possibilities of application to signal processing in the microwave band [4]–[6]. In a magnetized YIG film in the plane, if the bias magnetic field is perpendicular to the wave vector of MSW, then the MSSW propagates, while if the magnetic field is parallel to the wave vector, the MSBVW does. For the case that the magnetic field is neither perpendicular, nor parallel, in other words, in an obliquely magnetized YIG film, both MSSW and MSBVW modes propagate, which is called the MSSW/MSBVW mode, and the characteristics of such an MSSW/MSBVW mode continuously changes depending on the angle of magnetization [4], [7], [8].

Conventionally, the MSW excitation was calculated under the assumption that the current density distribution flowing in transducers was of uniform magnitude over the width of the transducers [9], [10]. However, this conventional method cannot be used to obtain a good approximation for any case.

The useful method to analyze exactly the excitation of MSWs is to solve the current density in transducers by means of numerical analysis methods. Some attempts in particular cases were made by several researchers [11], [12]. The advantages of the integral kernel expansion method are that we can formulate the MSW excitation problem elegantly, and that we can solve them formally for wide cases.

In this paper, we will analyze the excitation by a microstrip transducer on the in-plane and obliquely magnetized YIG by letting the current density be an unknown function and numerically solving it by means of the integral kernel expansion method. In order to verify the validity of the present method, we will then compare our numerical results with the experimental ones.

II. Theoretical Analysis

A. Formulation of the Problem

We consider the geometrical configuration of the present problem, as shown in Fig. 1, the upper panel of which is the top view and the lower one is the cross-sectional view.

The metal strip having the width $2w$ and the infinitesimal thickness is constructed on a YIG film with thickness d. The metal plane exists at $y = -d-h$ as the ground conductor of the microstrip transducer. The layer configuration goes infinitely along y- and z-directions, and the field is assumed to be

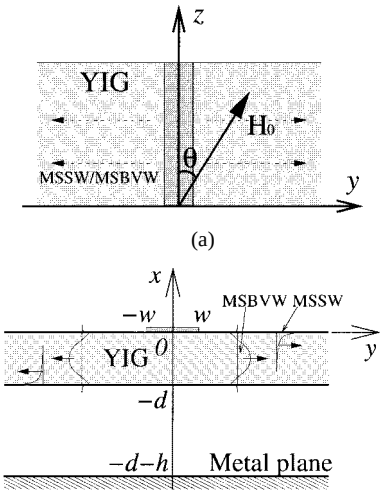

Fig. 1. Configuration for analysis.

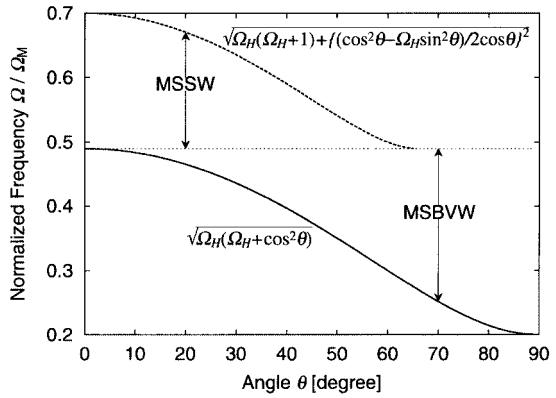

Fig. 2. MSW band characteristics changing the angle θ.

independent of z or $\partial/\partial z = 0$. The external direct magnetic field is applied in the direction making an angle θ with the z-axis, and then the MSW propagates in the $\pm y$-direction, as shown in Fig. 1, and also some examples of the potential profiles of both modes are drawn in Fig. 1(b). In this case, the following MSW modes can propagate depending on θ:

1) MSSW propagates for the magnetization perpendicular to the wave vector of MSW ($\theta = 0°$);
2) MSBVW, for the magnetization parallel to the wave vector ($\theta = 90°$);
3) MSSW/MSBVW, which propagates for the oblique magnetization of the YIG film ($0° < \theta < 90°$).

Fig. 2 shows the θ dependence of the frequency band of the MSSW/MSBVW. The ordinate is the normalized frequency $\Omega = \omega/\gamma M$, where ω, γ, and M are the angular wave frequency, gyromagnetic ratio, and saturation magnetization of the YIG, respectively, and the abscissa is the angle θ of the direct magnetic field. The magnitude of the applied magnetic field H is set as $\gamma H/\gamma M \equiv \Omega_H = 0.2$. The lower cutoff frequency of the MSBVW is given by $\sqrt{\Omega_H(\Omega_H + \cos^2\theta)}$ (the solid curve in Fig. 2), and decreases with the increase of θ. The dotted line indicates the upper cutoff frequency of the MSBVW and also the lower cutoff frequency of the MSSW, which are equal to $\sqrt{\Omega_H(\Omega_H + 1)}$. The upper cutoff frequency of the MSSW is given by

$$\sqrt{\Omega_H(\Omega_H+1) + \left(\frac{\cos^2\theta - \Omega_H \sin^2\theta}{2\cos\theta}\right)^2}$$

(the broken curve), which also decreases, and merge into the lower cutoff at the $\theta = \cot^{-1}\sqrt{\Omega_H}$, which is the called the critical angle of the MSSW.

From the configuration, a pair of Fourier transforms between the space and wavenumber domains is defined as follows:

$$f(y) = \int_{-\infty}^{\infty} \tilde{f}(k) e^{-jky}\, dk \tag{1}$$

$$\tilde{f}(k) = \frac{1}{2\pi}\int_{-\infty}^{\infty} f(y) e^{jky}\, dy. \tag{2}$$

It is assumed that magnetostatic approximation $\nabla \times \boldsymbol{H} = \boldsymbol{J}$ is valid and that the time factor is $\exp(j\omega t)$. The permeability tensor of in-plane magnetized YIGs is given by

$$\overline{\boldsymbol{\mu}}_r = \begin{bmatrix} \mu & -j\kappa_2 & j\kappa_3 \\ j\kappa_2 & \mu_2 & \mu_3 \\ -j\kappa_3 & \mu_3 & \mu_4 \end{bmatrix} \tag{3}$$

where

$$\begin{aligned} \kappa_2 &= \kappa\cos\theta \\ \kappa_3 &= \kappa\sin\theta \\ \mu_2 &= \mu\cos^2\theta + \sin^2\theta \\ \mu_3 &= (1-\mu)\cos\theta\sin\theta \\ \mu_4 &= \mu\sin^2\theta + \cos^2\theta \\ \mu &= 1 - \frac{\Omega_H}{\Omega^2 - \Omega_H^2} \\ \kappa &= \frac{\Omega}{\Omega^2 - \Omega_H^2}. \end{aligned}$$

With the use of the usual boundary conditions that the tangential component of the magnetic field and the normal component of magnetic flux density are continuous, we can obtain the relation between the current density flowing in the metal strip $J_z(y)$ and the magnetic flux density $B_x(y)$ on the $x = 0$-plane, in the wavenumber domain

$$\tilde{B}_x(k) = j\mu_0 G(k)\tilde{J}_z(k) \tag{4}$$

where

$$G(k) = -s\frac{N_0(k)}{D_0(k)} \tag{5}$$

$$\begin{aligned} N_0(k) =& (\mu q - \kappa_2 s)(\mu q + \kappa_2 s + \tanh|k|h) \\ & - (\mu q + \kappa_2 s)(\mu q - \kappa_2 s - \tanh|k|h)e^{-2q|k|d} \end{aligned} \tag{6}$$

$$\begin{aligned} D_0(k) =& (\mu q - \kappa_2 + 1)(\mu q + \kappa_2 + \tanh|k|h) \\ & - (\mu q + \kappa_2 - 1)(\mu q - \kappa_2 - \tanh|k|h)e^{-2q|k|d} \end{aligned} \tag{7}$$

and $q = \sqrt{\mu_2/\mu}$, $s = k/|k|$. It is noted that the function $G(k)$ has a pole in $k > 0$ and $k < 0$, respectively.

Taking the inverse Fourier transform and considering that $B_x(y) = 0$ in the metal strip region ($-w \leqq y \leqq w$) lead to the following equation:

$$\int_{-\infty}^{\infty} G(k)\tilde{J}_z(k)e^{-jky}\,dk = 0, \qquad -w \leqq y \leqq w. \quad (8)$$

This Fourier integral contains the unknown current density $\tilde{J}_z(k)$, and we can solve (8) by using the integral kernel expansion method.

B. Integral Kernel Expansion Method

First, the integral kernel of (8), e^{-jky}, is expanded into a series of the Legendre polynomials over the interval $-w \leqq y \leqq w$

$$e^{-jky} = \sum_{m=0}^{\infty} A_m(k)P_m\left(\frac{y}{w}\right). \quad (9)$$

The expansion coefficients $A_m(k)$ can be determined as follows. If we now multiply both sides of the above equation by $P_n(y/w)$, integrate over $-w$ to w, and invoke the orthogonality of the Legendre polynomials, we then obtain

$$\int_{-w}^{w} P_n\left(\frac{y}{w}\right)e^{-jky}\,dy = A_n\int_{-w}^{w}\left\{P_n\left(\frac{y}{w}\right)\right\}^2 dy \quad (10)$$

by changing the variables $y = wx$

$$\int_{-1}^{1} P_n(x)e^{-jkwx}\,dx = A_n\int_{-1}^{1}\left\{P_n(x)\right\}^2 dx. \quad (11)$$

The normalization integral of the Legendre polynomials is equal to $2/(2n+1)$, and the left-hand side can be rewritten in terms of the Rodrigues' formula [13]:

$$P_n(x) = \frac{(-1)^n}{2^n n!}\frac{d^n}{dx^n}\left[\left(1-x^2\right)^n\right]. \quad (12)$$

Integrating n times by parts, we obtain

$$\begin{aligned}\frac{2A_n}{2n+1} &= \frac{(-1)^n}{2^n n!}\int_{-1}^{1}\frac{d^n}{dx^n}\left[\left(1-x^2\right)^n\right]e^{-jkwx}\,dx\\ &= \frac{(-1)^n}{2^n n!}\left\{\left[\frac{d^{n-1}}{dx^{n-1}}\left[\left(1-x^2\right)^n\right]e^{-jkwx}\right]_{-1}^{1}\right.\\ &\qquad \left. +jkw\int_{-1}^{1}\frac{d^{n-1}}{dx^{n-1}}\left[\left(1-x^2\right)^n\right]e^{-jkwx}\,dx\right\}\\ &\qquad \vdots\\ &= \frac{(-jkw)^n}{2^n\,n!}\int_{-1}^{1}(x^2-1)^n e^{-jkwx}\,dx\\ &= (-j)^n 2\sqrt{\frac{\pi}{2kw}}\,J_{n+(1/2)}(kw)\\ &= (-j)^n 2j_n(kw) \end{aligned} \quad (13)$$

where $J_n(z)$ and $j_n(z)$ are the cylindrical and spherical Bessel functions, respectively, and we used the Poisson's integral for the Bessel function at the last of the above arrangement [14]. Consequently, we obtain

$$e^{-jky} = \sum_{m=0}^{\infty}(-j)^m(2m+1)j_m(kw)P_m\left(\frac{y}{w}\right). \quad (14)$$

Substituting (14) into (8) and invoking orthogonality of the Legendre polynomials, we can obtain

$$\int_{-\infty}^{\infty} G(k)\tilde{J}_z(k)j_m(kw)\,dk = 0, \qquad m = 0, 1, \ldots. \quad (15)$$

Next, we expand the unknown function $J_z(y)$ into a series of orthogonal polynomials with unknown coefficients

$$J_z(y) = \left\{1-\left(\frac{y}{w}\right)^2\right\}^{-(1/2)}\sum_{n=0}^{\infty} a_n T_n\left(\frac{y}{w}\right)\Pi\left(\frac{y}{w}\right) \quad (16)$$

where

$$\Pi(x) = \begin{cases} 1, & |x| \leqq 1 \\ 0, & |x| > 1 \end{cases}$$

and $T_n(z)$ is the Chebyshev polynomial and $a_n (n = 0, 1, \ldots)$'s are the unknown coefficients to be determined. The Fourier transform of (16) is given by

$$\tilde{J}_z(k) = \frac{w}{2}\sum_{n=0}^{\infty} a_n j^n J_n(kw). \quad (17)$$

Substituting (17) into (15), we can reduce the Fourier integral containing the unknown function into linear equations with respect to the unknown coefficients

$$\begin{bmatrix} L_{00} & L_{01} & \cdots & L_{0n} \\ L_{10} & L_{11} & \cdots & L_{1n} \\ \vdots & \vdots & & \vdots \\ L_{m0} & L_{m1} & \cdots & L_{mn} \end{bmatrix}\begin{bmatrix} a_0 \\ a_1 \\ \vdots \\ a_n \end{bmatrix} = 0 \quad (18)$$

where

$$L_{mn} = j^n w\int_{-\infty}^{\infty} G(k)j_m(kw)J_n(kw)\,dk \quad (19)$$

which can be calculated numerically, and we can then determine the coefficients a_n's to obtain the current density in (16) and (17).

The major difference from the spectral-domain method [15], [16] and the advantages of this method are the flexibility to choose the expansion functions of both the integral kernel and solution function, and the rapid convergence of the solution. We can choose the expansion function of the solution taking into account the physical condition for rapid convergence, which, as well as the function $G(k)$ in (8), limits a little the choice of the expansion function of the integral kernel, as noted below. However, the convergence of the integral kernel expansion is quickly obtained, e.g., in (14) for $kw = 1$, the expansion converges at $m = 4$, and if $kw = 6$, it converges at $m = 11$.

It is noted that when adopting the integral kernel expansion method, the choice of the polynomials expanding the integral kernel is necessarily limited by the function expanding the so-

lution because the integrals corresponding to (19) have to be bounded for any combination of m and n. The integrand of (19) decreases on the order of $k^{-(3/2)}$ so that the integrals are bounded. If we expand the integral kernel in terms of the Chebyshev polynomials T_m, the expansion would be given by

$$e^{-jky} = J_0(kw) + 2\sum_{m=1}^{\infty}(-j)^m J_m(kw) T_m\left(\frac{y}{w}\right) \tag{20}$$

and the resulting integrals L_{mn}'s would not converge at finite values for a particular combination of m and n because the integrand decreases on the order of k^{-1}.

C. Numerical Calculation of L_{mn}

Calculation of the infinite integrals of (19) is not straightforward because the integrands oscillate and also have pole singularities. In this section, we describe the techniques to overcome these difficulties.

Consider the integral over the positive k given by

$$w\int_0^{\infty} G(k) j_m(kw) J_n(kw)\, dk = \int_0^{\infty} G\left(\frac{z}{w}\right) j_m(z) J_n(z)\, dz. \tag{21}$$

As $k \to +\infty$, the function $G(k)$ approaches exponentially to the constant G^+ as follows:

$$G^+ = -\frac{\mu q - \kappa_2}{\mu q - \kappa_2 + 1}. \tag{22}$$

Thus, we separate the integral into two parts as follows:

$$L_{mn}^{+} = \int_0^{\infty}\left\{G\left(\frac{z}{w}\right) - G^+\right\} j_m(z) J_n(z)\, dz + G^+\int_0^{\infty} j_m(z) J_z(z)\, dz. \tag{23}$$

$G(z/w) - G^+$ can be deformed as follows:

$$G\left(\frac{z}{w}\right) - G^+ = \frac{N(z)}{D(z)} \tag{24}$$

where

$$N(z) = \left\{(\mu q + \kappa_2)(\mu q - \kappa_2 + 1) - (\mu q - \kappa_2)(\mu q + \kappa_2 - 1)\right\} \times \frac{\left(\mu - \kappa_2 - \tanh z\frac{h}{w}\right) e^{-2qzd/w}}{(\mu q - \kappa_2 + 1)} \tag{25}$$

$$D(z) = (\mu q - \kappa_2 + 1)\left(\mu q + \kappa_2 + \tanh z\frac{h}{w}\right) - (\mu q + \kappa_2 - 1)\left(\mu q - \kappa_2 - \tanh z\frac{h}{w}\right) e^{-2qzd/w}. \tag{26}$$

It is found here that the integrand of the first term of (23) vanishes exponentially and the convergence of the numerical computation can be obtained easily.

We still have another difficulty, which is the pole singularities, as we mentioned before. Here, we explain how to process them in the computation. The preliminary definitions are introduced for convenience of notation as follows:

$$R(z) = sN(z) j_m(z) J_n(z) \tag{27}$$

$$D'(z) = \frac{dD(z)}{dz}. \tag{28}$$

In order to evaluate the contribution of the poles of $N(z)/D(z)$, we subtract the singularities from the integrand and add the compensating term. Letting the pole $z_+ = k_+ w$, we have

$$\int_0^{\infty}\frac{R(z)}{D(z)}\, dz = \int_0^{\infty}\left\{\frac{R(z)}{D(z)} - \frac{R(z_+)}{D'(z_+)}\frac{\exp\left(-\frac{z-z_+}{z_+}\right)}{z - z_+}\right\} dz + \frac{R(z_+)}{D'(z_+)}\int_0^{\infty}\frac{\exp\left(-\frac{z-z_+}{z_+}\right)}{z - z_+}\, dz. \tag{29}$$

The compensating term, or the second term of (29), can be evaluated by the Cauchy principal value of the integral and half the residue, i.e.,

$$\int_0^{\infty}\frac{\exp\left(-\frac{z - z_+}{z_+}\right)}{z - z_+}\, dz = \mathrm{PV}\int_0^{\infty}\frac{\exp\left(-\frac{z - z_+}{z_+}\right)}{z - z_+}\, dz - i\pi \tag{30}$$

where PV stands for the principal value of the integral, and the second term has the minus sign because, with the loss of the medium, the pole z_+ would be located below the real axis in the complex z-plane. The principal value of the integral can be estimated as follows:

$$\mathrm{PV}\int_0^{\infty}\frac{\exp\left(-\frac{z-z_+}{z_+}\right)}{z - z_+}\, dz = \mathrm{PV}\int_{-1}^{\infty}\frac{\exp(-\zeta)}{\zeta}\, d\zeta = -\overline{Ei}(1) = -1.895117816\ldots \tag{31}$$

where $\overline{Ei}(\zeta)$ is the exponential integral function.

The second term of (23) can be calculated analytically, and the result is given by

$$\frac{\pi\Gamma\left(\frac{m+n+1}{2}\right) G^+}{2\Gamma\left(\frac{m-n+2}{2}\right)\Gamma\left(\frac{n-m+1}{2}\right)\Gamma\left(\frac{m+n+2}{2}\right)}. \tag{32}$$

Note that the result is identically equal to zero when $n - m - 2$ or $m - n - 1$ is positive and even.

It is noted that the integration over the negative half-infinite interval can be done in a similar manner.

D. Derivation of Equations for Comparison With Experiments

We can observe the excitation of MSWs as the loss of transmission lines and, in the present problem, we measure the $|S_{21}|$ of the scattering matrix of the microstrip line in Fig. 1. In this

section, we derive the equations for the sake of comparison with experimental data.

By using the Poynting vector, the average power flow per unit length along with the $\pm y$-direction is given by

$$P_{\pm} = -\frac{2\pi^2\mu_0\omega\left|\tilde{J}_z(k_{\pm})\right|^2}{k_{\pm}D'^2(k_{\pm})} \times \left[\frac{N_0^2(k_{\pm})}{2|k_{\pm}|} + \left(K_{+}T_{mm}^2e^{-2q|k_{\pm}|d} + K_{-}T_{pp}^2\right) \times \frac{1-e^{-2q|k_{\pm}|d}}{2q|k_{\pm}|} + 2\mu_2T_{mm}T_{pp}e^{-2q|k_{\pm}|d}\,d + 2(\mu q)^2e^{-2q|k_{\pm}|d}\left\{\frac{h}{\cosh^2|k_{\pm}|h} + \frac{\tanh|k_{\pm}|h}{|k_{\pm}|}\right\}\right] \tag{33}$$

where the sign $\pm$ represents the $\pm y$-direction of the power flow, respectively, and

$$K_{\pm} = \mu q \pm \kappa_2 s \tag{34}$$

$$T_{pp} = \mu q + \kappa_2 s + \tanh|k_{\pm}|h \tag{35}$$

$$T_{mm} = \mu q - \kappa_2 s - \tanh|k_{\pm}|h \tag{36}$$

$$D'(k) = s(\mu q - \kappa_2 s + 1)\frac{h}{\cosh^2|k|h} + s(\mu q + \kappa_2 s - 1)e^{-2q|k|d} \times \left\{\frac{h}{\cosh^2|k|h} + 2qd(\mu q - \kappa_2 s - \tanh|k|h)\right\}. \tag{37}$$

The total current is obtained by integrating (16) directly over the metal strip, i.e.,

$$I = \int_{-w}^{w} J_z(y)\,dy = \pi w a_0. \tag{38}$$

Thus, the radiation resistance of the transducer is given by

$$R = \frac{2(P_{+} - P_{-})}{|I|^2} \tag{39}$$

and the radiation reactance is obtained by taking the Hilbert transform of the radiation resistance

$$X(\omega) = \frac{1}{\pi}\,\mathrm{PV}\int_{-\infty}^{\infty}\frac{R(\omega')}{\omega' - \omega}\,d\omega'. \tag{40}$$

Finally, assuming that the loss of the transmission line is negligible, we obtain the following attenuation constant α_{att}:

$$\alpha_{\mathrm{att}} = \sqrt{\frac{-\omega C(\omega L + X) + \sqrt{\{\omega C(\omega L + X)\}^2 + (\omega CR)^2}}{2}} \tag{41}$$

where $\omega L = \beta Z$ and $\omega C = \beta/Z$ and C, L, Z, and β are the line capacitance, line inductance, characteristic impedance, and propagation constant of the transducer, respectively.

III. Numerical and Experimental Results

First, we calculate the insertion loss of the microstrip transducer, which is regarded as the energy transformed into MSSWs. Figs. 3 and 4 show the numerical results estimated by the present method (as denoted by the solid lines) and by the conventional ones, which are based on the following assumed current distributions $J_z(y)$.

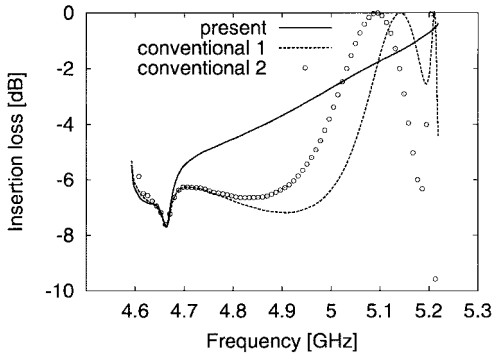

Fig. 3. Numerical results on the frequency dependence of $|S_{21}|$ for $\theta = 0°$. The results by the present method are denoted by a solid line and those by the conventional method are denoted by a dotted line.

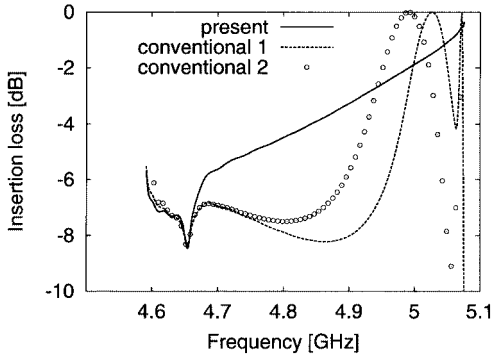

Fig. 4. Same numerical results as Fig. 3, but for the case of $\theta = 20°$.

1) $J_z(y)$ is constant in the strip, i.e.,

$$J_z(y) = \frac{1}{2w}, \qquad |y| \leqq w \tag{42}$$

$$\tilde{J}_z(k) = \frac{1}{2\pi}\,\frac{\sin kw}{kw} \tag{43}$$

and the results are denoted by dotted lines.

2) $J_z(y)$, whose field singularities at both edges of the metal strip are added [17], i.e.,

$$J_z(y) = \frac{1}{\pi w}\,\frac{1}{\sqrt{1 - \left(\dfrac{y}{w}\right)^2}}, \qquad |y| \leqq w \tag{44}$$

$$\tilde{J}_z(k) = \frac{1}{2\pi}\,J_0(kw) \tag{45}$$

with the results denoted by circles. Note that the assumed current distribution 2 corresponds to the present method only with the term of the zeroth order ($n = 0$).

These are calculated for the case of $\theta = 0°$ (for which the upper cutoff frequency of the MSSW is 5.22 GHz) and $\theta = 20°$ (5.08 GHz), respectively. The parameters used in the calculations are $d = 20$ μm, $h = 500$ μm, $w = 62.5$ μm, $H_0 = 77.6$ kA/m, $M = 141.7$ kA/m, and the length of the transducer

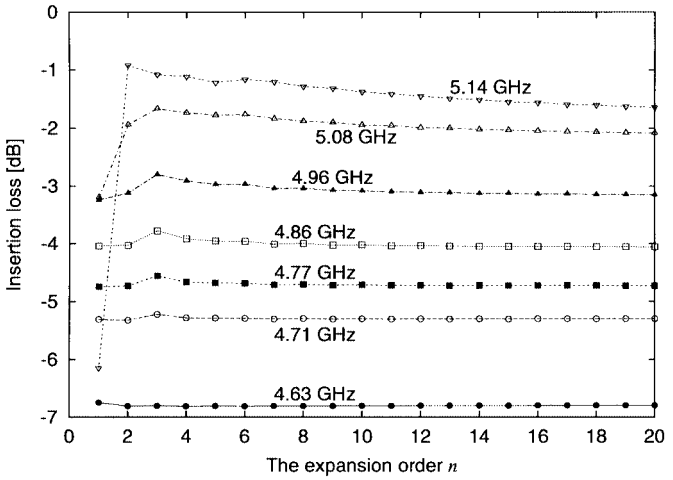

Fig. 5. Convergence of the numerical results.

is 8 mm. We truncate the expansion with respect to n in (17) by ten terms and to m in (14) by twice n.

From these figures, we can observe the considerable differences between the results computed by the present method and by both of the conventional methods over the frequencies of our interest.

Second, we show the dependences of numerical convergence on the number of expansion terms with frequency as a parameter in Fig. 5 in order to examine the convergence of computing results because we have to truncate the expansion of (14) and (17) by the finite terms for carrying out numerical calculation. It is noted that $n = 1$ in the abscissa means the expansion of the unknown function (16) consists of two terms ($n = 0$ and 1). All data are for the case of $\theta = 0°$. It is seen that we have convergence with the increase in n and we can see that it is sufficient for convergence to truncate the expansion by approximately seven terms over almost all of the frequency range, but at the upper frequencies, the convergence is relatively slow. This is because the approximate solution expanded into the finite series of the Bessel functions approaches the exact solution from low frequencies and the terms with the Bessel functions of the higher order contribute to it at upper frequencies. However, almost over the main range of the MSSW band, the convergence is obtained by the expansion of a few terms.

Experiments were performed to verify the validity of the present theory. Using a vector network analyzer (HP8720C), we measured the $|S_{21}|$ of the transducer or the insertion loss.

Fig. 6 shows the schema of the device-under-test. The YIG used in this experiment is 20-μm thick, 24-mm wide, and 10-mm long. Both edges of the YIG are rough by rasping to prevent the straight-edge resonance. We construct the metal strip directly on the YIG surface by evaporating aluminum. The dimensions of the metal strip is shown in Fig. 6(b): 1-mm-wide and 1-mm-long parts in the both sides for transition between SMA connectors and the transducer, and 125-μm-wide center part for the transducer, i.e., $w = 62.5$ μm in Fig. 1. The distance between the metal strip and ground plane is approximately 500 μm, for which the characteristic impedance and effective dielectric constant of this transmission line are approximately 208.0 Ω and 6.20, respectively, if the YIG is regarded just as a

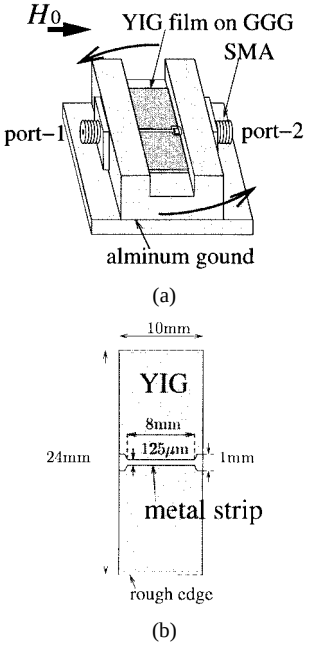

Fig. 6. Configuration of the device-under-test.

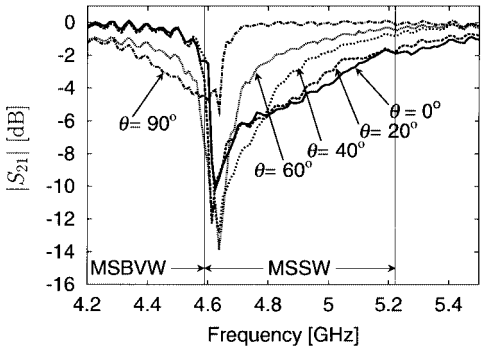

Fig. 7. Frequency dependence of S_{21} of the test device for various values of the angle of the magnetic field (θ).

dielectric. The YIG film is directly mounted on the aluminum ground plane, which is rotatable on the aluminum support and can be fixed at any angles. The aluminum support is fixed by the equipment applying a direct magnetic field.

Fig. 7 shows the experimental results of the frequency dependence of $|S_{21}|$ of the transducer when we changed the angle of the biased magnetic field θ with a constant magnitude of 77.6 kA/m ($= 975$ Oe). The frequency where the MSSW exists for $\theta = 0°$ is found to range from 4.59 to 5.22 GHz, and the corresponding frequency band for the MSBVW ($\theta = 90°$) propagation is in a range from 2.73 to 4.59 GHz. It is known that with an increase in θ, the upper limit of the MSSW band shows a decrease and the lower limit of the MSBVW band becomes lower [4], [7], [8], and such a tendency can actually be found in Fig. 7.

In Figs. 8–10, we plot the experimental and numerical results by the present method for the case of $\theta = 0°$, 20°, and 30°, and also the results by the conventional method for comparison. All three of these figures clearly suggest that the frequency dependences by the present method exhibit the behaviors much closer

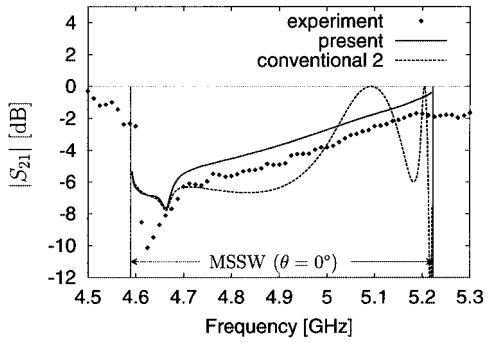

Fig. 8. Comparison of the experimental results (denoted by dots) with the numerical computations in the case of $\theta = 0°$. The full line refers to the numerical results by the present method. We also plot the ones by the conventional method (dotted line) for comparison.

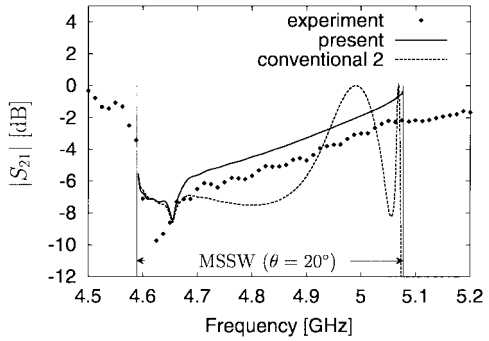

Fig. 9. Same as Fig. 8, but for the case of $\theta = 20°$.

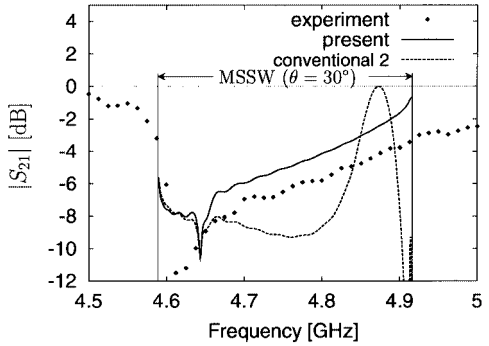

Fig. 10. Same as Fig. 8, but for the case of $\theta = 30°$.

to the experimental frequency dependences than those by the conventional analysis method.

Even though the present method has yielded considerably better agreement with the experimental result than the previous conventional result, we still notice a significant discrepancy between the two, which should be seriously discussed. In the frequency band of the MSSW, the experimental data are seen from these figures to indicate a greater loss of approximately 1 dB than the numerical results by the present method. This difference can be accounted for by the undesirable return loss at the transition between the coaxial and microstrip line, radiation into free space, and/or conductive loss of the metal strip. It is also found from these figures that extra excitation exists out of the MSSW band. It seems to be due to the inhomogeneity of the applied magnetic field and the demagnetization in the fringes of the YIG film.

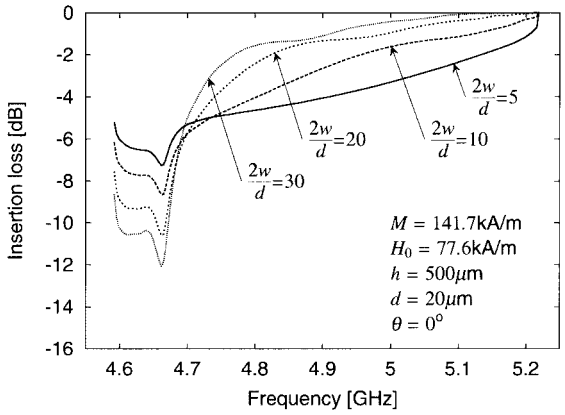

Fig. 11. Calculated frequency characteristics of the MSSW excitation changing the ratio of strip width to YIG thickness $2w/d$. The data are calculated by the integral kernel expansion method.

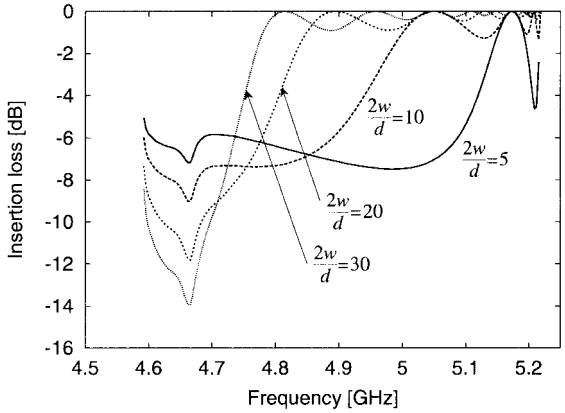

Fig. 12. Same as Fig. 11, but calculated by the conventional method adopting the uniform current distribution. The parameters used for computation are the same as in Fig. 11.

Here, we shall consider the dependence of the MSSW excitation on the microstrip geometry by means of the developed method in this study. We change the ratio of strip width to YIG thickness $2w/d$ as a parameter, while the others are fixed, as shown in Fig. 11. The necessary values for the computation are written in the graph. We can see that, as the ratio $2w/d$ increases, the excitation in the lower frequency range becomes stronger, while the one in the higher range does weaker gradually.

We also show the calculated results by the conventional method to use the uniform current distribution for reference in Fig. 12. The same tendency of dependence on the ratio $2w/d$ is as shown in the previous figure, but the difference from the present method is large in the high-frequency range when the ratio is low, i.e., the strip is narrow. In [10], it is mentioned that the agreement between the calculation with the uniform current and the experiment is poor for the narrow strip. Consequently, although the uniform current approximation can be applicable for wide strip transducers, it is necessary to use our developed method for excitation analyses for narrow strip transducers. Moreover, with taking into account that narrow strip transducers would be important for MSW devices to require broad excitation, we can conclude that the present method would be highly useful and should be used in the analysis.

IV. Conclusion

We have presented the integral kernel expansion method, which is an integral-equation solver, as the application to analysis of the MSSW excitation in the in-plane magnetized YIG film. This method allows us to formulate the present problem elegantly and solve it successively. The agreement of the numerical results by the present method with the corresponding experiment is generally good, while there is still a significant discrepancy between the conventional ones and the experiment. It has been evident that the integral kernel expansion method used in this paper is appropriate for the analyses of MSW excitation problems.

References

[1] N. Guan, K. Yashiro, and S. Ohkawa, "Integral kernel expansion method for mixed boundary value problems in electromagnetic field theory," *J. Fac. Eng. Chiba Univ.*, vol. 48, no. 1, pp. 29–38, 1996.

[2] Y. Ando, N. Guan, K. Yashiro, and S. Ohkawa, "Excitation of magnetostatic surface wave by coplanar waveguide transducers," *IEICE Trans. Electron.*, vol. E81-C, no. 12, pp. 1942–1947, 1998.

[3] ——, "Excitation of magnetostatic surface waves by slot line transducers," *IEICE Trans. Electron.*, vol. E82-C, no. 7, pp. 1123–1128, 1999.

[4] R. W. Damon and J. R. Eshbach, "Magnetostatic modes of a ferromagnet slab," *J. Phys. Chem. Solid*, vol. 19, pp. 308–320, 1961.

[5] W. S. Ishak, "Magnetostatic wave technology: A review," *Proc. IEEE*, vol. 76, pp. 171–187, Feb. 1988.

[6] C. S. Tsai, "Integrated acoustooptic and magnetooptic devices for optical information processing," *Proc. IEEE*, vol. 84, pp. 853–869, June 1996.

[7] M. J. Hurben and C. E. Patton, "Theory of magnetostatic waves for in-plane magnetized isotropic films," *J. Magn. Magn. Mater.*, vol. 139, pp. 263–291, 1995.

[8] Y. Ando, N. Guan, K. Yashiro, and S. Ohkawa, "Effects of a metal plane on MSSW/MSBVW modes in a YIG film," in *INTERMAG '99 Dig.*, Kyongju, Korea, Paper BE-06.

[9] A. K. Ganguly and D. C. Webb, "Microstrip excitation of magnetostatic surface waves: Theory and experiment," *IEEE Trans. Microwave Theory Tech.*, vol. MTT-23, pp. 998–1006, Dec. 1975.

[10] A. K. Ganguly, D. C. Webb, and C. Banks, "Complex radiation impedance of microstrip-excited magnetostatic-surface waves," *IEEE Trans. Microwave Theory Tech.*, vol. MTT-26, pp. 444–447, June 1978.

[11] P. R. Emtage, "Generation of magnetostatic surface waves by a microstrip," *J. Appl. Phys.*, vol. 53, no. 7, pp. 5122–5125, 1982.

[12] G. A. Vugal'ter and V. N. Makhalin, "Reflection and excitation of magnetostatic surface waves by a metal strip," *Sov. Phys. Tech. Phys.*, vol. 30, no. 3, pp. 296–300, 1985.

[13] E. T. Whittaker and G. N. Watson, *A Course of Modern Analysis*. Cambridge, U.K.: Cambridge Univ. Press, 1965, p. 303.

[14] G. N. Watson, *A Treatise on the Theory of Bessel Functions*. Cambridge, U.K.: Cambridge Univ. Press, 1966, p. 48.

[15] T. Itoh and R. Mittra, "Spectral-domain approach for calculating the dispersion characteristics of microstrip lines," *IEEE Trans. Microwave Theory Tech.*, vol. MTT-21, pp. 496–499, July 1973.

[16] Q. Zhang and T. Itoh, "Spectral-domain analysis of scattering from E-plane circuit elements," *IEEE Trans. Microwave Theory Tech.*, vol. MTT-35, pp. 138–150, Feb. 1987.

[17] R. E. Collin, *Field Theory of Guided Waves*, 2nd ed. New York: IEEE Press, 1991, pp. 23–28.

Yoshiaki Ando (M'00) was born in Tokyo, Japan, on May 12, 1972. He received the B.E., M.E., and Ph.D. degrees in electrical and electronics engineering from Chiba University, Chiba, Japan, in 1995, 1997, and 2000, respectively.

Since 2000, he has been with the Department of Electronic Engineering, The University of Electro-Communications, Tokyo, Japan, where he is currently a Research Associate. His research interests are MSWs and computational electromagnetics of natural phenomena.

Ning Guan (M'89) was born in Hunan, China, in 1962. He received the B.S., M.S., and Ph.D. degrees in electrical and electronics engineering from Chiba University, Chiba, Japan, in 1985, 1987, and 1990, respectively.

From 1991 to 2000, he was a Research Associate with the Department of Electronics and Mechanical Engineering, Chiba University, where he was involved with magnetostatic-wave devices, theory of propagation of electromagnetic waves, and applications of wavelet to boundary value problems in electromagnetic theory. Since 2000, he has been with the Optics and Electronics Laboratory, Fujikura Ltd., Chiba, Japan. His current research interests are the analysis of optical fibers and design of planar lightwave circuits.

Ken'ichiro Yashiro (M'83) received the B.E. and M.E. degrees in electronics engineering from Chiba University, Chiba, Japan, in 1974 and 1976, respectively, and the D.E. degree from the Tokyo Institute of Technology, Tokyo, Japan, in 1979.

In 1979, he joined the Department of Electrical and Electronics Engineering, Chiba University, where he was a Research Associate. He became an Associate Professor in 1987 and a Full Professor in 1998. His research interests include magnetostatic-wave devices, magnetic solitons, electromagnetic-wave scattering, and inverse scattering problems.

Sumio Ohkawa (SM'81) was born in Hokkaido, Japan, on July 16, 1935. He received the B.Eng. degree in electrical engineering from Chiba University, Chiba, Japan, in 1961, and the D.Eng. degree from the Tokyo Institute of Technology, Tokyo, Japan, in 1974.

He then joined the Department of Electrical Engineering, Chiba University, as an Associate Professor, and in 1978, became a Full Professor. From October 1979 to July 1980, he was a Visiting Professor with the Microwave Research Institute, Polytechnic Institute of New York. In 2001, he was appointed Professor Emeritus with Chiba University. His research has mainly concerned measurements of materials in the microwave range. He is currently also interested in applications of magnetostatic-wave devices and magnetostatic-wave envelope solitons.

Masashi Hayakawa received the B.E., M.E., and D.Eng. degrees from Nagoya University, Nagoya, Japan, in 1966, 1968, and 1974, respectively.

In 1970, he joined the Research Institute of Atmospherics, Nagoya University, as a Research Associate. In 1968, he became an Assistant Professor, and in 1969, he became an Associate Professor. Since 1991, he has been a Professor with The University of Electro-Communications, Tokyo, Japan. He is Co-Editor of *Radio Science*. His interests include space plasma waves, atmospheric electricity, seismo-electromagnetics, electromagnetic compatibility (EMC), and inversion problems.

Dr. Hayakawa is a member of the America Geophysical Union, International Scientific Radio Union (URSI), Institute of Electrical, Information and Communication Engineers (IEICE), Japan, the Institute of Electronics Engineers Japan, the Society of Atmospheric Electricity of Japan, and the Society of Geomagnetism and Earth, Planetary and Space Sciences. He was the URSI Commission E chair (1996–1999). He is currently the President of the Society of Atmospheric Electricity of Japan. He is on the Technical Program Committee of the Zurich EMC Symposium and also on the Scientific Program Committee of Wroclaw EMC Conference.